Increased long-latency reflex activity as a sufficient explanation for childhood hypertonic dystonia: a neuromorphic emulation study

2015 J. Neural Eng. 12 036010

(http://iopscience.iop.org/1741-2552/12/3/036010)

IOP Publishing Journal of Neural Engineering
J. Neural Eng. 12 (2015) 036010 (14pp) doi:10.1088/1741-2560/12/3/036010

Increased long-latency reflex activity as a sufficient explanation for childhood hypertonic dystonia: a neuromorphic emulation study

Won J Sohn[1,5], Chuanxin M Niu[4,5] and Terence D Sanger[1,2,3]

[1] Department of Biomedical Engineering, University of Southern California, 1042 Downey Way, Los Angeles, CA 90089, USA
[2] Department of Biokinesiology, University of Southern California, 1042 Downey Way, Los Angeles, CA 90089, USA
[3] Department of Neurology, University of Southern California, 1042 Downey Way, Los Angeles, CA 90089, USA
[4] Department of Rehabilitation, Ruijin Hospital, School of Medicine, Shanghai Jiao Tong University, Shanghai, People's Republic of China

E-mail: tsanger@usc.edu

Received 28 October 2014, revised 6 February 2015
Accepted for publication 27 March 2015
Published 7 May 2015

Abstract

Objective. Childhood dystonia is a movement disorder that interferes with daily movements and can have a devastating effect on quality of life for children and their families. Although injury to basal ganglia is associated with dystonia, the neurophysiological mechanisms leading to the clinical manifestations of dystonia are not understood. Previous work suggested that long-latency stretch reflex (LLSR) is hyperactive in children with hypertonia due to secondary dystonia. We hypothesize that abnormal activity in motor cortices may cause an increase in the LLSR leading to hypertonia. *Approach.* We modeled two possibilities of hyperactive LLSR by either creating a tonic involuntary drive to cortex, or increasing the synaptic gain in cortical neurons. Both models are emulated using programmable very-large-scale-integrated-circuit hardware to test their sufficiency for producing dystonic symptoms. The emulation includes a joint with two Hill-type muscles, realistic muscle spindles, and 2,304 Izhikevich-type spiking neurons. The muscles are regulated by a monosynaptic spinal pathway with 32 ms delay and a long-latency pathway with 64 ms loop-delay representing transcortical/supra-spinal connections. *Main results.* When the limb is passively stretched, both models produce involuntary resistance with increased antagonist EMG responses similar to human data; also the muscle relaxation is delayed similar to human data. Both models predict reduced range of motion in voluntary movements. *Significance.* Although our model is a highly simplified and limited representation of reflex pathways, it shows that increased activity of the LLSR is by itself sufficient to cause many of the features of hypertonic dystonia.

Keywords: neuromorphic, reflex, dystonia, electromyograph (EMG), motor control

(Some figures may appear in colour only in the online journal)

[5] The authors equally contributed to the study.

1. Introduction

Dystonia is an involuntary alteration in the pattern of muscle activation during voluntary movement or maintenance of posture (Sanger *et al* 2003). In secondary dystonia, symptoms are often caused by injury to cortex, thalamus or basal ganglia (Colton *et al* 2002, Sanger *et al* 2003, Breakefield *et al* 2008), but the link between injury to these areas and the resulting clinical symptoms remains unclear. Previous work suggested that the long-latency stretch reflex (LLSR) is abnormally increased in childhood hypertonia due to secondary dystonia (Kukke and Sanger 2011). We do not know whether the elevated LLSR is a cause of dystonia or merely an associated phenomenon. To explore this question, we test using simulation whether elevation of LLSR in a highly simplified model is sufficient to cause features of hypertonic dystonia, including resistance to passive stretch, delayed muscle relaxation, and reduced range of motion in voluntary movement.

The eventual manifestation of secondary dystonia may be attributable to increased activity in the motor cortex. Brain imaging provides the direct evidence of increased motor cortical activity in secondary dystonia (Ceballos-Baumann 1994); other studies using transcranial magnetic stimulation over motor cortex also show increased corticospinal excitability (Trompetto *et al* 2012, Kojovic *et al* 2013). In other forms of dystonia, it was found that patients exhibit reduced intracortical inhibition (Ridding *et al* 1995, Edwards *et al* 2003, Quartarone *et al* 2003, Prescott *et al* 2013) and increased cortical plasticity (Quartarone *et al* 2003, Edwards *et al* 2006, Weise *et al* 2006, Prescott *et al* 2013). The association between increased motor cortex activity and secondary dystonia could be due to an inhibitory effect of basal ganglia over motor cortex, possibly through thalamocortical pathways (DeLong and Wichmann 2007, Hallett 2011). This association is supported by clinical treatments for patients of dystonia, where dystonic symptoms were alleviated after ablative surgeries (Imer *et al* 2005, Hashimoto *et al* 2010) or deep brain stimulations (McIntyre *et al* 2004, Vidailhet *et al* 2005, Krauss 2010, Air *et al* 2011) in the globus pallidus internus. Therefore in this emulation study we focus on how different cortical parameters lead to abnormal reflex behaviors similar to dystonia.

One possible outcome of increased motor cortex excitability is to elevate LLSR due to the role of primary motor cortex in reflex modulation (Evarts and Tanji 1976, Lee *et al* 1983, Morimoto *et al* 1984, Capaday *et al* 1991, Matthews 1991, Palmer and Ashby 1992, Pruszynski *et al* 2011). Therefore loss of inhibition in the motor cortex may leak an uncontrolled drive that either lowers the threshold of cortical cells or amplifies their response to afferent input. In both cases the activity of LLSR is expected to increase. In our previous studies, children with secondary dystonia showed increased reflex activity (van Doornik *et al* 2009) with long-latency responses (Kukke and Sanger 2011), which could potentially cause hypertonia in this population. Taken together, existing evidence suggests that the hypertonic manifestation of secondary dystonia may be directly caused by elevated LLSR, which potentially results from many insults including increased motor cortex excitability after injuries in basal ganglia, cerebellum, thalamus, or sensory cortices.

To determine whether this is a plausible mechanism for hypertonic dystonia and not merely an epiphenomenon, we emulate the effect of increased cortical drive or increased afferent input to cortex. The term 'emulation' is used to disambiguate from numerical simulations (usually slower than real-time) in software. We do not include a model of the basal ganglia, because we seek to test whether any structure projecting to and causing uncontrolled firing of motor cortical areas could potentially be a cause of dystonia. Other possible areas with oligosynaptic connectivity to motor cortices include prefrontal cortex, primary sensory cortex, thalamus, and cerebellum. We choose the synthetic analysis approach primarily because it allows flexible ways of introducing abnormalities that are physiologically plausible but difficult to obtain from human subjects in laboratory. It also provides information about physiological components at drastically different physical and temporal scales, including millisecond time-scale action potentials in microscopic neurons, and seconds-long contractions in whole muscles. We leverage the recently available technology of programmable very-large-scale-integrated-circuit (VLSI), which allows us to create emulations of neurons that communicate using spikes, with the ability to increase the number of emulated neurons without sacrificing speed. With VLSI, the neural circuitry and connectivity is also easily modifiable. In this study, we first built a small set of structures to create a non-impaired system with functioning reflexes including a short-latency loop representing the spinal monosynaptic reflex pathway, and a long-latency loop representing the supra-spinal/transcortical pathway. Due to the aforementioned contribution of motor cortex to long-latency response, we selectively increase the activity of the transcortical pathway to emulate a hyperactive LLSR. We hypothesize two possible causes of hyperactive LLSR. First, the cortical neurons may receive a tonic drive that is either sub- or supra-threshold but overall depolarizing. This TONIC model makes the cortical neurons easier to fire or achieve high firing rate, even when receiving the same level of excitatory post-synaptic current (EPSC) from sensory feedback. Second, the synaptic gain of cortical neurons may uniformly increase, which augments the excitability of cortical neurons. This HI-GAIN model amplifies the EPSC provided by ascending sensory feedback, which eventually elevates the overall activity of the transcortical pathway. These two mechanisms are the major categories of abnormality that can lead to increases in LLSR at the cellular level, so we modeled both. We argue it is important to test if different mechanisms are both sufficient to produce dystonia, which may eventually help sub-categorizing secondary dystonia. In both models, the spinal pathway remains intact and therefore only the long-latency component in the reflex pathway is elevated.

We focus on changes in EMG or movement kinematics by comparing both TONIC and HI-GAIN models with the non-impaired condition. There are three experiments in this study:

(1) passive back-and-forth stretch,
(2) voluntary relaxation of force,
(3) voluntary back-and-forth movement.

In the first two experiments, data from human subjects are available and thus compared to verify the sufficiency of our model for producing dystonia; human data are not yet available for the last experiment, therefore the results can be used as testable hypotheses for future experiments.

2. Materials and methods

We focus on using spike-based emulation to determine the functional role of sensorimotor components, especially their sufficiency for causing clinical symptoms in abnormal conditions. The hardware emulation of the spiking neurons and sensorimotor components is constructed using field programmable gate arrays (FPGA, Xilinx Spartan-6), a programmable version of VLSI electronic chips. We favor FPGAs over pipelined hardware such as graphic processing units or clustered central processing units due to their inherent parallelism that resembles neural circuitry. We also found that when networking multiple units for large-scale disease emulation, FPGAs allow significantly more flexibility than custom-built hardware for communication protocols such as neuromorphic transmission protocols that directly transmit neuron-like spikes.

The activity of the emulated sensorimotor system is recorded using a dedicated data-logging computer. The FPGA communicates with the data-logging computer through a high-speed USB channel and the OpalKelly development kit and interface software (XEM6010, OpalKelly Inc.). The technical details can be located in the previous study (Niu *et al* 2014). The biomechanics of the limb is simulated in software. The biomechanical simulation updates its states by first polling muscle force from the FPGAs, followed by sending muscle kinematic variables (length and velocity of lengthening) back to the FPGAs. This hybrid setup containing both hardware and software is slower than pure hardware emulation, but it simplifies the coordination between flexor and extensor FPGA chips.

2.1. Models for the sensorimotor system and increased LLSR

We study a sensorimotor system that includes a limb joint comprising two opposing monoarticular muscles (flexor and extensor), muscle spindles, spindle afferents, alpha-motoneurons and associated supraspinal structures (figure 1(A)). The hardware emulates parallel proprioceptive pathways including monosynaptic connections with 32 ms loop-delay representing the spinal proprioceptive pathway, and oligosynaptic pathways with 64 ms loop-delay representing the supra-spinal/transcortical components of the stretch reflex loop. The delays were chosen both to approximate known conduction delays and also for efficiency of hardware emulation. Our previous work suggests that in sensorimotor systems, the statistical effect of two fully connected neuron populations is equivalent to ones that are only sparsely connected (Sanger 2011), therefore we connect the spindle afferents to motoneurons using parallel connections instead of implementing the full connectivity among neurons. In this study we do not introduce inhibitory mechanisms such as Renshaw cells or reciprocal inhibition. Both gamma dynamic and gamma static drive are set to 80 Hz, which is a moderate intensity of fusimotor stimulus in the classic experiment chosen for modeling the muscle spindle (Emonet-Denand *et al* 1977). No alpha–gamma coactivation is introduced. This provides a baseline system for the non-impaired behavior before introducing the disease model.

On top of the non-impaired system, we model two possible mechanisms to increase LLSR: the TONIC model and HI-GAIN model. In the TONIC model (figure 1(B)), we superimpose a tonic input on the voluntary commands via a depolarizing synapse. The tonic input lowers the threshold of the cortical neuron pool and therefore facilitates the transcortical pathway when stimulated by proprioceptive feedback. In the HI-GAIN model (figure 1(C)), the synaptic gain of afferent inputs to the cortical neuron pool is increased by augmenting the excitatory postsynaptic potential (EPSC) in response to afferent input. Therefore the TONIC model is an additive excitatory drive that is present even in the absence of afferent input, while the HI-GAIN model is a multiplicative drive that is present only when afferent input is present. Both TONIC and HI-GAIN models increase the excitability of cortical neuron pools to afferent input, either by lowering threshold or by increasing the effect of the input. We test both models because either or both mechanisms could be active in childhood dystonia.

2.2. Implementation of sensorimotor system on hardware

An adult elbow joint is simulated in software as a 34 cm beam freely rotating around a single DOF axis, the mass of the beam is 1.52 kg as an approximation to a human fore arm (Scheidt and Ghez 2007); the moment arm of muscle is simplified as constant 30 mm, which is in the middle range of moment arm measured from human biceps (Murray *et al* 1995). The joint is driven by a pair of antagonistic muscles following Hill-type model (Hill 1938). The sensorimotor components that interact with the simulated joint are arranged on FPGA hardware as shown in figure 2. Each muscle is controlled by 128 spindles as modeled by Mileusnic *et al* (2006), simple spiking neurons developed by Izhikevich (Izhikevich 2003), and a motor-unit action potential model similar as (Fuglevand *et al* 1993, Rodriguez *et al* 2007, Krutki *et al* 2008) producing a surface electromyogram. Izhikevich neurons are used because they permit use of biologically realistic variables including transmembrane currents, yet they can be implemented much more efficiently in hardware than the more complex Hodgkin–Huxley equations that they approximate. A total of 768 alpha-motoneurons were divided into six groups representing motor units with various sizes, so that the size principle (Henneman *et al* 1965) is present when motor units are recruited. The parameters are tuned such that at maximal spiking rate of the alpha-motoneuron pool, the

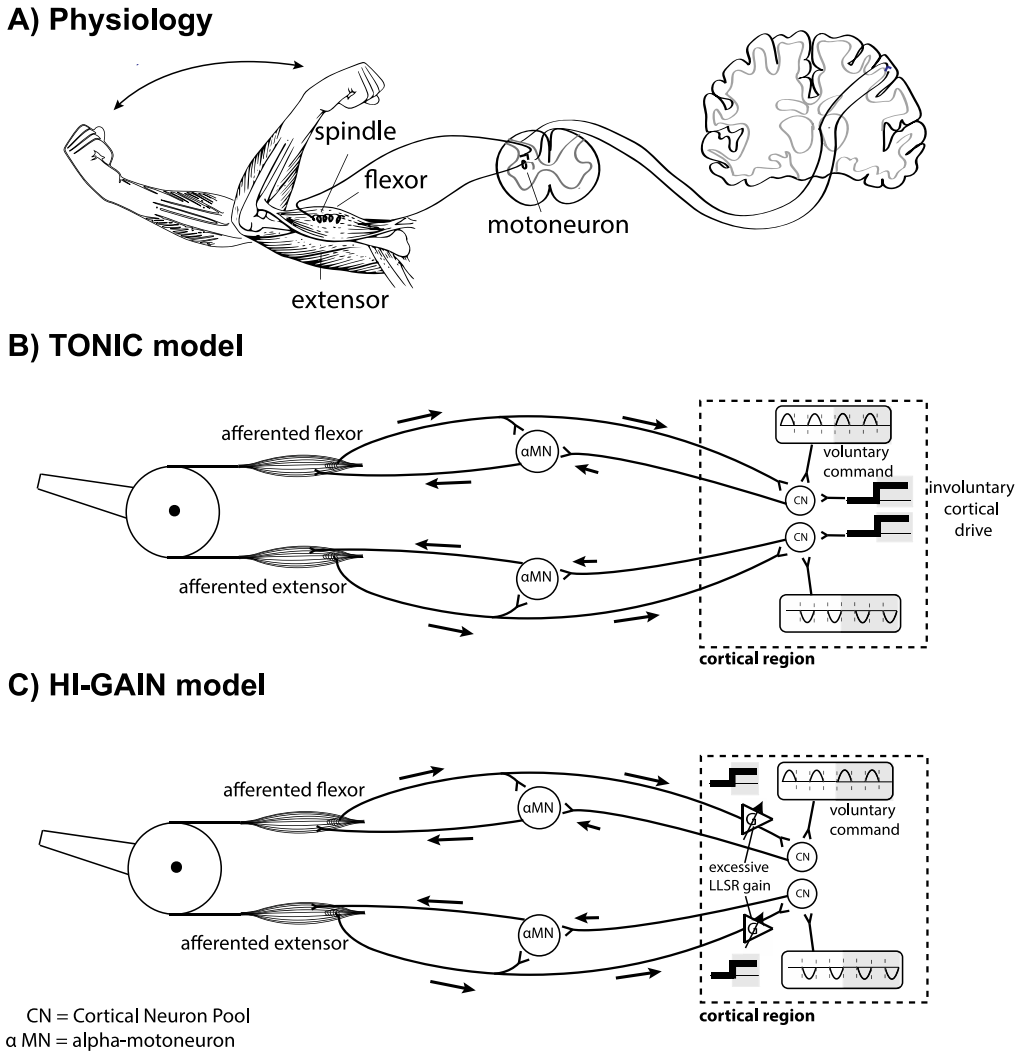

Figure 1. (A) Components of human sensorimotor system model. The system includes a limb joint comprising two opposing monoarticular muscles (flexor and extensor), muscle spindles, spindle afferents, alpha-motoneurons, and associated spinal and supraspinal structures. Our model includes a monosynaptic reflex arc with a 32 ms loop-delay and a supra-spinal transcortical reflex pathway with a 64 ms loop-delay. (B) The TONIC model of dystonia. The dashed box shows the procedure of introducing involuntary *tonic* activity. Before the disease onset (unshaded area), the system executes the voluntary commands received from antagonistic cortical inputs; after the disease onset (shaded area), the voluntary descending commands are superimposed on a tonic input. (C) The HI-GAIN model of dystonia. The synaptic gain associated with the afferent cortical projection becomes higher after the disease onset (shaded areas), which directly increases the loop-gain of the transcortical feedback loop.

muscle exerts approximately 5 N tangential force at the tip of the joint. In the transcortical loop, the spindle afferent information travels through a population of 128 cortical neurons representing the primary sensory and motor cortices. The main focus of modeling cortex is to enable a longer loop-delay compared to spinal pathways, therefore we accept a pool of 128 neurons as a model of cortex even though it is a clear oversimplification of the real biology. Due to the limited capacity of each FPGA unit, the system must be distributed on multiple FPGAs as indicated by the blocks. The entire system uses six interconnected FPGA boards to emulate two muscles and 2,304 spiking neurons.

2.3. Experiments

We have verified the sufficiency of both the TONIC and HI-GAIN models for dystonic symptoms in the following three experiments:

2.3.1. Experiment 1: passive back-and-forth stretch. We replicate the experiment where a sinusoidal perturbation was applied to a joint of a child with hypertonic arm dystonia (van Doornik *et al* 2009). In the original study, the subject was instructed to rest, and the right arm was rotated manually by the experimenter following an approximately sinusoidal time profile with frequency varying from 0.2 up to 2 Hz.

We use the same waveform as in the original study to stretch the emulated system. A pre-recorded waveform of joint displacement is applied to the software-simulated joint. We keep the voluntary command at zero during the passive stretch to capture the fact the subject was at rest. It was found that patients with dystonia failed to relax the muscles and produced cyclic EMG responses to the stretch. The models of dystonia are validated based on their abilities to qualitatively explain human data. To this purpose, we calculate the phase angle between the model-generated EMG and the joint angle

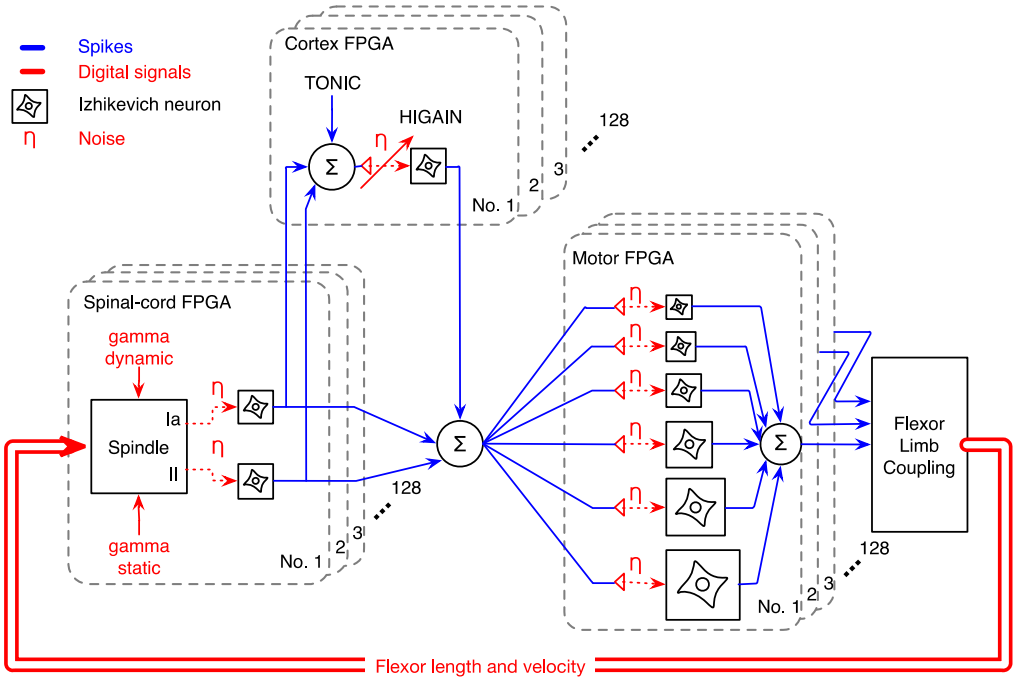

Figure 2. Detailed configuration of the motor nervous system on neuromorphic hardware. The components are implemented separately for the flexor and extensor, which simultaneously drive the joint modeled as a beam freely rotating around the endpoint (simulated in software outside FPGAs). For each muscle (flexor or extensor), the muscle force is calculated from a Hill-type muscle model activated by six motoneuron pools with six different motoneuron sizes, each pool comprising of 128 identical motoneurons modeled by Izhikevich (Izhikevich 2003). The motoneuron pools receive excitatory input from both the spinal loop and transcortical loop. In the spinal loop, the sensory feedback is provided by muscle spindles implemented as Mileusnic and colleagues did (Mileusnic *et al* 2006), which include both the primary (Ia) and secondary (II) afferents to provide the dynamic and static proprioceptive information about the muscle. A total of 128 spindles are implemented for each muscle, thus providing 256 independently spiking afferents. In the transcortical loop, the spindle afferents synapse on a population of 128 cortical neurons representing the primary sensory and motor cortex. The cortical part is clearly an oversimplification of the cortex but it enables an additional 32 ms conduction delay in the proprioceptive feedback loop, which is the main focus of this study rather than modeling a full cortex. In the cortex, spindle afferents may join additional inputs modeling the voluntary motor command. The TONIC model is implemented by adding to the cortical drive a tonic component that is independent from the voluntary drive or the sensory feedback. The HI-GAIN model is implemented by increasing the synaptic gain of the spindle afferents prior to activating the cortical neuron pool. Due to the limited capacity of each FPGA unit, the system must be distributed on multiple FPGAs as indicated by the blocks. The entire system uses six FPGA boards enabling two muscles with 2,304 neurons. Only half of the system (flexor) is shown.

using the same approach as in van Doornik *et al* (2009). The range of phase angle reflects which kinematic variable could be the main cause of the EMG response. For example, a phase angle of 0° means the EMG response is in line with the joint angle, thus making the EMG position-dependent; while −90° means the EMG response is velocity-dependent; any phase angle between −180° and −90° suggests that the EMG response has acceleration-dependent components; any phase angle between 0° and 180° means that the EMG is active during muscle shortening.

During model validation, we first introduce a small TONIC input (TONIC model) to the cortical neuron pool or a small cortical gain (HI-GAIN model) sufficient to produce dystonic symptoms, i.e. an observable phase angle. Then we progressively increase the intensity of dystonia until the phase angle stopped changing significantly, mainly due to the saturation of neurons. We consider a model sufficient to explain human data if the parameter-scan produces a wide range of phase angle that includes those from human patients.

2.3.2. Experiment 2: voluntary relaxation of muscle. One of the common manifestations of childhood dystonia is that the voluntary relaxation of muscle contraction is delayed (Sanger *et al* 2003). We replicate the experiment that documented this delay by comparing normal subjects to patients with secondary dystonia (Ghez *et al* 1988).

Both muscles were first activated at 50% maximum voluntary contraction, followed by a step decrease in the voluntary command. This experiment simulated when the subject attempts to rapidly relax the co-contracted muscles following a cue signal (Ghez *et al* 1988). It was shown that the EMG decreased more slowly in patients with secondary dystonia, and thus the overall duration of muscle relaxation was delayed.

We quantify the rate of muscle relaxation by fitting the filtered EMG to a sigmoid function defined below:

$$\mathrm{EMG}_{\mathrm{sigmoid}}(t) = \mathrm{EMG}_{\mathrm{min}} + \frac{\left(\mathrm{EMG}_{\mathrm{max}} - \mathrm{EMG}_{\mathrm{min}}\right)}{1 + \mathrm{e}^{\tau t}},$$

where the free parameter τ denotes the rate at which the EMG decreases during muscle relaxation. The relationship between τ and the severity of dystonia was tested using a similar parameter-scan as in Experiment 1.

2.3.3. Experiment 3: reduced range of motion in voluntary movements. In clinic, it is commonly observed that patients with dystonia apply great efforts in order to achieve a normal range of movement; otherwise the range of motion in voluntary movements is reduced. These phenomena are, however, not well documented in experimental studies. It is reported that the range of motion is reduced in neck and knee for patients with primary dystonia (Carpaneto *et al* 2004, Lebiedowska *et al* 2004). We hypothesize that similar reduction in range of motion is likely to occur in secondary dystonia. In addition, we test if the reduced range of motion can be improved by amplifying the voluntary command, which is a straightforward engineering approach to compensate a less responsive system.

The two cortical neuron pools regulating flexor and extensor receive half-wave rectified sinusoidal waveforms (180° out of phase), which produces a back-and-forth joint swinging movement. The peak-to-peak amplitudes of joint angle resulting from these inputs are analyzed. If the amplitude of joint angle is reduced in dystonia models, we linearly increase the sinusoidal voluntary commands to test if the reduction can be compensated.

2.4. Data acquisition and processing

All data are sampled at 1 kHz. The EMG signals are first high-pass filtered using 10 Hz cut-off frequency (Butterworth, third order), followed by rectification and a low-pass filter at 120 Hz cut-off frequency (Butterworth, third order). Phase angle analysis and the nonlinear fitting of the sigmoid function (for quantifying muscle relaxation, explained below) are performed using Matlab (Mathworks, Inc.).

3. Results

3.1. Non-impaired stretch reflex and hypertonia with increased LLSR

We first verify the quality of emulation by passively stretching the joint and monitoring the reflex behavior elicited by the stretch. The joint was passively extended by 45° within 0.2 s from the software interface. The sensorimotor information recorded in response to a virtual stretch in the non-impaired condition is shown in figure 3(A), including the spindle afferents (group Ia and II), motoneuron rasters, muscle force and EMG. As can be seen, the hardware emulation is capable of producing concurrent multi-scale information during a virtual behavior.

We further compared the stretch reflex between the non-impaired condition and our two dystonia models. The joint was briefly stretched using a short torque pulse (5 N for 20 ms, figure 3(B)), which extended the flexor by approximately 40% of L_0 (the resting length of muscle). Hypertonia can be seen from the increased flexor force in the dystonia conditions compared to the non-impaired condition (figure 3(B), muscle force). The EMG response is divided into R1 (30–50 ms), R2 (50–80 ms), and R3 (80–100 ms) regions representing the short-, long-, and longer-latency responses. By overlapping the non-impaired condition and our models of dystonia (figure 3(B), EMG), it can be seen that R2 responses are increased by both TONIC and HI-GAIN model, i.e. LLSR is increased in both models.

3.2. Experiment 1: involuntary responses to passive joint stretch

The dystonic subjects showed phasic EMG responses to the manual sinusoidal stretch in their biceps (figure 4(A)). In the emulation, the virtual arm was passively rotated with the identical waveform as shown in figure 4(A). Our emulated result showed that in both TONIC (figure 4(B)) and HI-GAIN (figure 4(C)) models, the flexor EMG activity modulates with the joint angle similarly to the original human experiment.

The eight patients with dystonia from human experiments (van Doornik *et al* 2009) showed a wide range of phase angle between −101° and 17° (table 2, van Doornik *et al* 2009). There were 2 patients (subjects 4 and 5) with dyskinetic cerebral palsy who showed positive phase angles, suggesting EMG responses during muscle shortening (a 'shortening reaction' more frequently seen in Parkinsonism). These two patients were excluded from the model validation, since their mechanisms were unlikely the same as the other six patients who were non-dyskinetic. As can be seen from figure 5, five out of six patients showed phase angles between −90° and 0° (combination of position- and velocity-dependent); one out of six patients showed a joint angle below −90° (with acceleration-dependent components).

We validate our models of dystonia by testing whether the reported phase angles in human can be achieved in emulation. In the TONIC model, we scan the tonic EPSC with fixed increments from 40 up to 280 pA. We stop at 280 pA since further increases did not significantly change the phase angle mainly due to the saturation of cortical neurons. The scan of tonic EPSC produces phase angles from −32°to −53°, which explains only one out of six patients (dark gray area, figure 5(A)). In the HI-GAIN model, we start the scan by selecting a unit gain that amplifies the non-impaired EPSC by four times, then we progressively increase the gain to 19 times of a unit. We stop at the gain of 19 for the same reason of saturation. This process produces phase angles from −29° to −147°, which covers the reported phase angles of all six subjects (dark gray area, figure 5(B)).

We infer the upper and lower limits of phase angle by setting the emulation to boundary conditions (light gray area in figure 5). The upper limit of phase angle is obtained by de-afferenting the secondary fibers (group II) and keeping the loop gain high; and the lower limit is obtained by de-afferenting the primary fibers (group Ia) and keeping the loop gain low. The boundary conditions are constructed based on the factors that may affect the phase shift, e.g. loop delay, loop

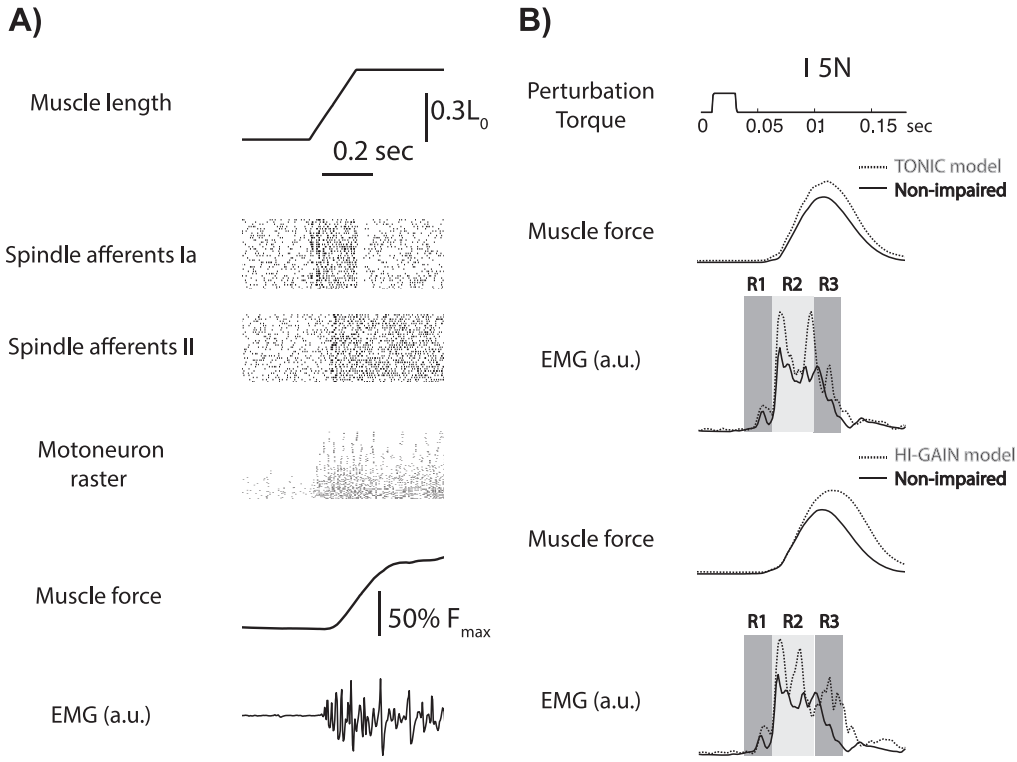

Figure 3. The emulated stretch reflex in the non-impaired condition and models of increased LLSR. (A) EMG responses to a stretch-and-hold perturbation in the non-impaired condition. The joint flexor was stretched by approximately 40% of L_0. The emulated EMG showed a burst in response to the stretch. The motoneuron raster showed patterns compatible with both the early burst in EMG response and the subsequent tonic components. (B) Emulated hypertonia and increased LLSR. The muscle force increases from baseline in both TONIC and HI-GAIN model, which implemented the increased muscle resistance to passive muscle stretch commonly observed in hypertonic dystonia. EMG responses to a torque pulse perturbation (5 N for 20 ms) in both the non-impaired condition and the models of dystonia. R1 (30–50 ms), R2 (50–80 ms), and R3 (80–100 ms) regions represent the short-, medium-, and long-latency responses. In both the TONIC and the HI-GAIN model the R2 response was increased compared with the non-impaired condition.

gain, and the relative contribution between position- and velocity-dependent components, etc, see section 4 for further considerations. The overall range of phase angle (−9° to −169°) is larger than both TONIC and HI-GAIN models.

The sensitivity of phase angle to the intensity of emulated dystonia in each model is shown in figure 6. In the TONIC model, the phase angle decreases with increased tonic current input following a significant linear correlation (figure 6(A), slope $= -0.074$, $p < 0.0001$, $r^2 = 0.59$, four repetitions for each level of TONIC input). In the HI-GAIN model, similar linear correlation is observed (figure 6(B), slope $= -6.50$, $p < 0.0001$, $r^2 = 0.78$, four repetitions for each level of HI-GAIN). Overall, the HI-GAIN model can capture more variance in phase angle than could the TONIC model. The results suggest that in terms of phase angle, the HI-GAIN model can explain more data than the TONIC model, although both models produce results qualitatively similar to the human data.

3.3. Experiment 2: delayed relaxation of muscle force

Figure 7 shows that both the TONIC and HI-GAIN models suffice to delay muscle relaxation compared with the non-impaired condition. The phenomenon is qualitatively similar to human data.

The rate of relaxation (τ) was calculated both from human data and emulated results for model validation. Due to the limited human data, we could only obtain two values of τ based on the original EMG time series in Ghez *et al* (1988). The τ calculated from the normal subject almost tripled that from the patient with secondary dystonia ($\tau_{\text{normal}} = 0.044$, $\tau_{\text{dystonia}} = 0.015$), which is compatible with the visual pattern of delayed relaxation (figure 7(A)). These two values of τ are plotted in figure 8 (dotted and dashed lines) for comparison with emulated τ.

In the TONIC model, the level of TONIC input was scanned using the same set-up as in experiment 1. The emulated τs were all lower than τ_{normal} (figure 8(A)), and τ_{dystonia} was included in the emulated range of τ. When the TONIC input increases, the delay of relaxation is significantly longer (slope $= -0.00012$, $p < 0.00001$, $r^2 = 0.65$, four repetitions for each level of TONIC input). In the HI-GAIN model, the emulated τs were also lower than τ_{normal} (figure 8(B)). But the linear correlation between τ and model intensity is much weaker, represented by modest significance and lower r^2 value (figure 8(B), slope $= -0.00051$, $p = 0.046$, $r^2 = 0.11$, four repetitions for each level of HI-

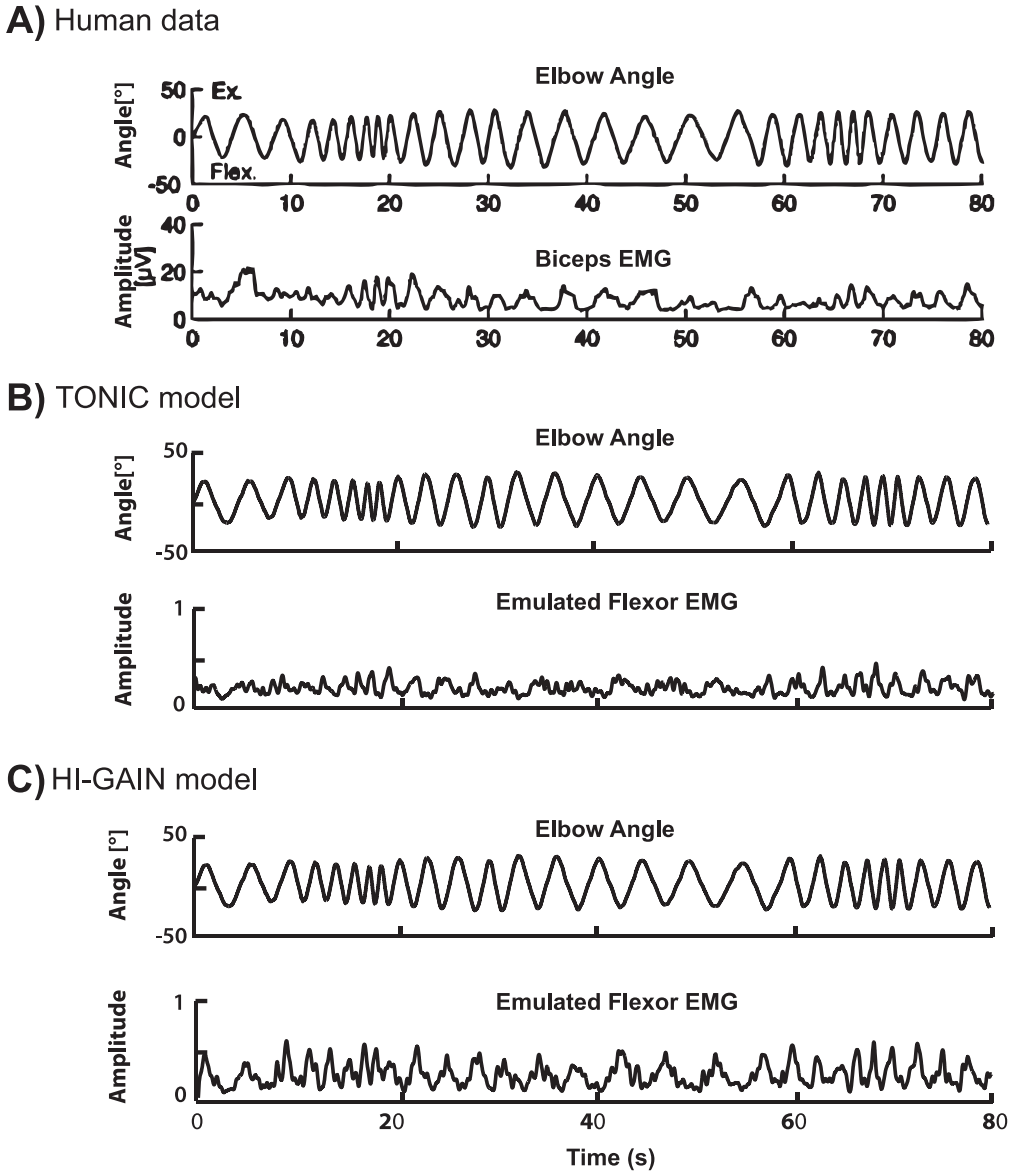

Figure 4. Biceps EMG during arm rotation in a child with hypertonic arm dystonia (A) created based on the data in van Doornik *et al* (2009). When the subject was instructed to rest, the right arm was rotated manually by the experimenter following approximately a sinusoidal time profile with frequency varying from 0.2 up to 2 Hz. The biceps showed phasic EMG responses to the manual stretch. In the emulation, the virtual joint was passively rotated with the identical waveform under two models of dystonia. The voluntary command is set to zero to represent the subject being 'at rest'. In the TONIC model (B), the EMG is not silent when the joint is passively rotated and shows similar phasic patterns as the human EMG recording. In the HI-GAIN model (C), similar non-silent EMG responses are observed with increased magnitude in phasic response.

GAIN). In contrast to experiment 1, results from experiment 2 suggest that the TONIC model can explain more data than the HI-GAIN model.

3.4. Experiment 3: reduced range of motion in voluntary movements

In this experiment, we aimed to predict how dystonia affects movement kinematics. In the TONIC model, just adding a middle level TONIC input is sufficient to reduce the peak-to-peak amplitude of voluntary movement (figure 9). The reduced range of motion can almost fully recover if we amplify the voluntary commands, suggesting that patients can compensate the reduced range of motion by increasing voluntary effort. Similar results are produced using the HI-GAIN model. In this experiment, both models predicted similar kinematic consequences using anecdotal parameters. More human data are required to distinguish between these two models.

4. Discussion

Using our recently developed technique of neuromorphic emulation in hardware, we tested the hypothesis that increased LLSR, created by excessive activity in the motor

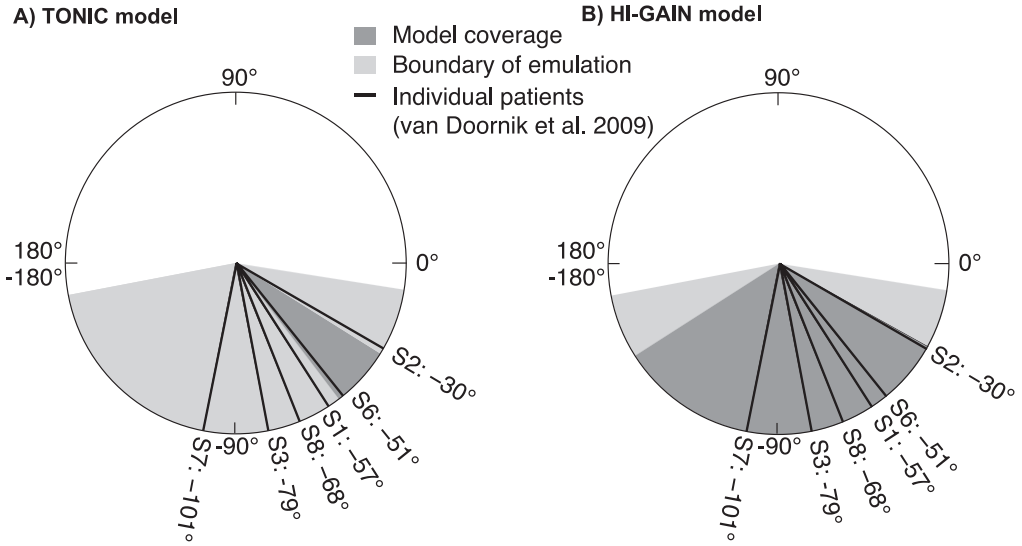

Figure 5. The phase angle calculated from emulation and human data. The thick lines show the phase angles of six patients with hypertonic arm dystonia. (A) The TONIC model produces phase angles from −32° to −53° (dark gray area), which includes one out of six patients. (B) The HI-GAIN model produces phase angles from −29° to −147° (dark gray area), which includes all six patients. The boundary of emulation is tested by de-afferenting either the primary (group Ia) or the secondary (group II) spindle fiber, resulting in the minimum phase angle of −169° and the maximum of −9° (light gray area).

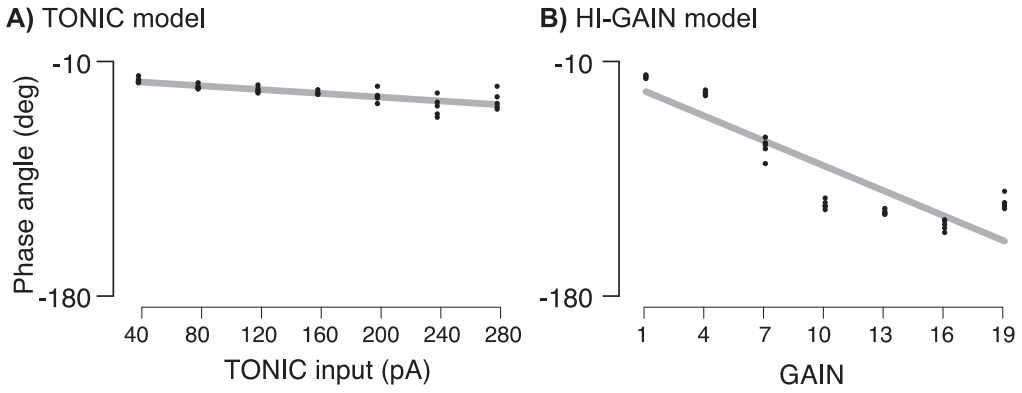

Figure 6. The sensitivity of phase angle to the intensity of emulated dystonia in each model. In the TONIC model, we scan the TONIC input from 40 to 280 pA with fixed increments. The average phase angles produced by these TONIC inputs range from −32° to −53°, where a higher TONIC input significantly reduces the phase angle (slope = −0.074, $p < 0.0001$, $r^2 = 0.59$, four repetitions for each level of TONIC input). The linear trend tends to saturate when the TONIC input exceeds 240 pA. In the HI-GAIN model, we start the scan of cortical gain by selecting a unit gain that amplifies the non-impaired EPSC by four times. The gain is increased to 19 times of a unit with fixed increments. The average phase angles produced by the HI-GAIN model range from −29° to -147°, where a higher cortical gain significantly reduces the phase angle (slope = −6.50, $p < 0.0001$, $r^2 = 0.78$, four repetitions for each level of HI-GAIN). The linear trend tends to saturate when the TONIC input exceeds 16 units. These results suggest that in terms of phase angle, the HI-GAIN model can explain more human data than the TONIC model.

cortex, are sufficient to induce forces and EMGs with similar patterns to those seen in patients with secondary dystonia. In particular, we verified that when the limb is passively stretched as in van Doornik *et al* (2009), both an additive tonic input in the cortical neuron pool (TONIC model) and an elevated synaptic gain in the motor cortex (HI-GAIN model) suffice to induce EMG responses in the absence of a voluntary command. The HI-GAIN model explains a wider range of phase angle from human data than does the TONIC model. Furthermore, we verified that both TONIC and HI-GAIN models suffice to delay muscle relaxation similar to the results of Ghez *et al* (1988). The rate of relaxation could be better explained by TONIC model than the HI-GAIN model. Our models also predict that the range of movement should be reduced if the magnitude of the voluntary command remains the same in dystonia. Alternatively, we predict that dystonia increases the voluntary effort required to make movements of the same magnitude.

4.1. Relationship between LLSR and secondary dystonia

Our results suggest that increased LLSR may be an intermediate mechanism linking brain injuries and the clinical manifestations of hypertonic dystonia. That is, even though the injuries may occur in various parts of the brain (e.g. thalamus, basal ganglia, cortex, etc), all these injuries could

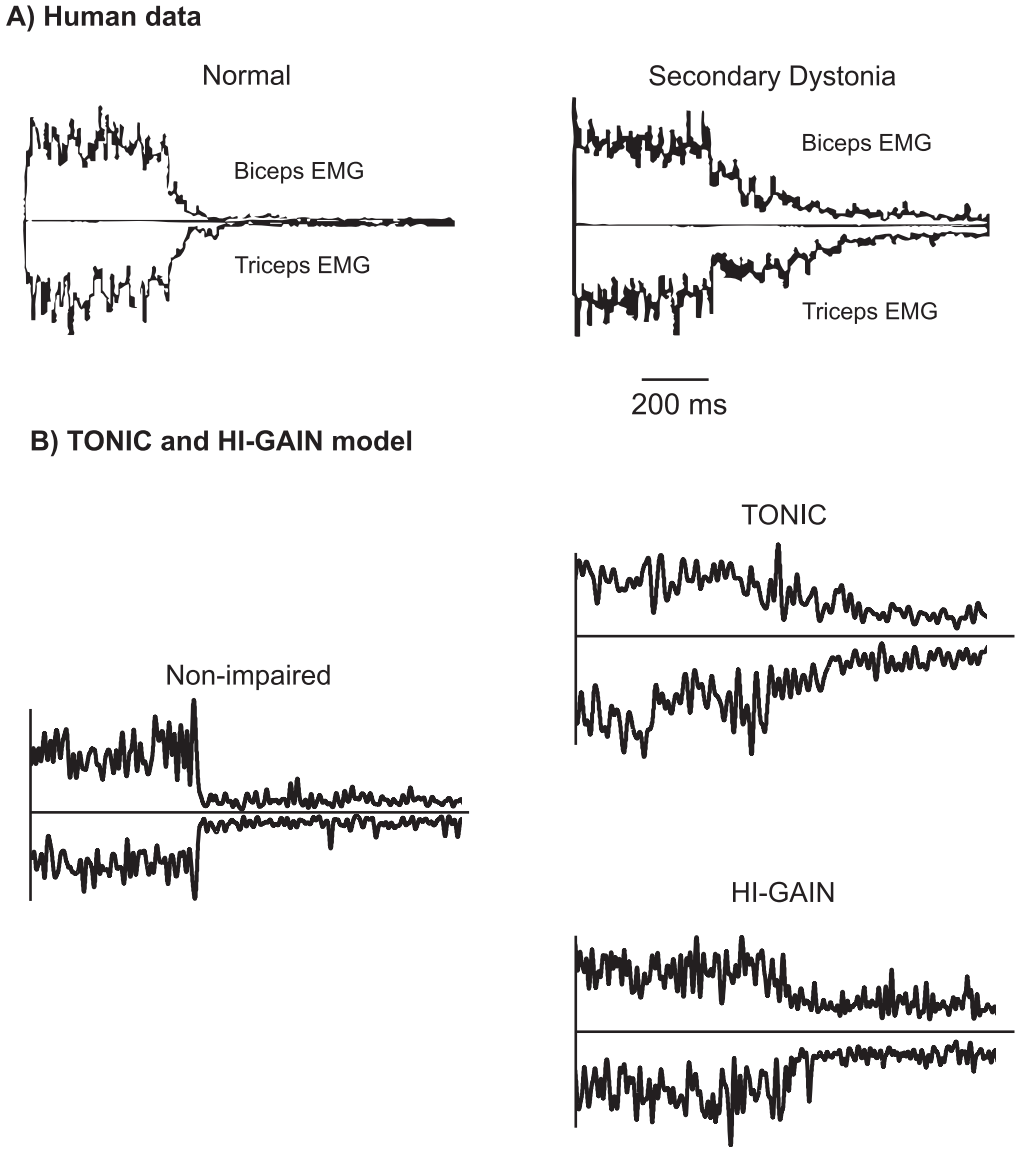

Figure 7. Relaxation of muscle activity from a state of co-contraction in biceps and triceps in a normal subject and a patient with secondary dystonia (A), created based on the data in Ghez *et al* (1988). Subjects were first required to maximally co-contract the biceps and triceps muscles and upon a visual cue relax the muscle as fast as possible. The duration for muscle relaxation in the patient with secondary dystonia (right) was elongated compared to the normal subject (left). In emulation (B), both TONIC and HI-GAIN models showed delayed EMG relaxation compared with the non-impaired condition, when the voluntary descending command that co-contracts biceps and triceps were abruptly shut off. Single representative trials are shown.

produce hypertonic dystonia due to excess activity in the motor cortex via elevated LLSR. We show that both TONIC and HI-GAIN models are sufficient for explaining the dystonic symptoms in the demonstrated cases. Nevertheless, the manifestation of these two models could differ when the severity of dystonia increases (figure 6); it is also suggested that hypertonia due to tonic input may have a stronger effect than high synaptic gain on the delay in muscle relaxation (figure 8). In theory, the TONIC model can be interpreted as a non-intrinsic abnormal drive to the motor cortex, originated from other parts of the brain; while the HI-GAIN model suggests that there is some intrinsic deficit in the motor cortex that amplifies its overall activity. These differences suggest testable hypotheses in future studies to distinguish the heterogeneous causes of dystonia.

Elevated LLSR is not exclusively observed in dystonia but also reported in other disorders such as rigidity. It is possible that dystonia and rigidity may share similarities in mechanism, although due to very different causes. It was not our intent to study rigidity, which is rare in children, but from our prior work (van Doornik *et al* 2009) we have noted that even within dystonia there appears to be a continuum between spring-like hypertonia and viscous hypertonia. Rigidity is primarily viscous and it is tempting to conjecture that rigidity may result from increased LLSR involving primarily velocity-dependent (rapidly adapting) afferents, whereas dystonia may

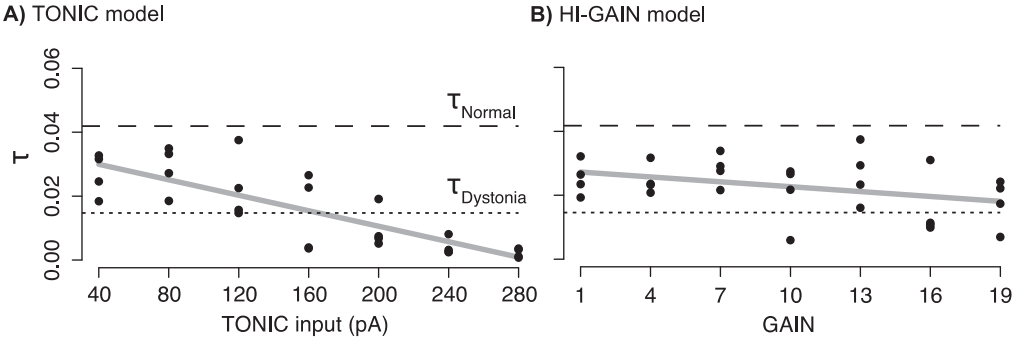

Figure 8. Relationship between the rate of relaxation (τ) and the intensity of either the TONIC or the HI-GAIN model. In both models, the intensity of dystonia is scanned the same as in experiment 1. Two reference αs calculated from human data are shown, the rate in the normal subject ($\tau_{normal} = 0.044$, dashed line) represents faster relaxation compared to the patient with secondary dystonia ($\tau_{dystonia} = 0.015$, dotted line). In the TONIC model (A), the emulated τs are all lower than τ_{normal}, and their range includes $\tau_{dystonia}$. When the TONIC input increases, the delay of relaxation is significantly longer (slope $= -0.00012$, $p < 0.00001$, $r^2 = 0.65$, four repetitions for each level of TONIC input). In the HI-GAIN model, the emulated τs are also lower than τ_{normal} (B). But the linear correlation between τ and model intensity is much weaker, represented by modest significance and lower r^2 value (slope $= -0.00051$, $p = 0.046$, $r^2 = 0.11$, four repetitions for each level of HI-GAIN).

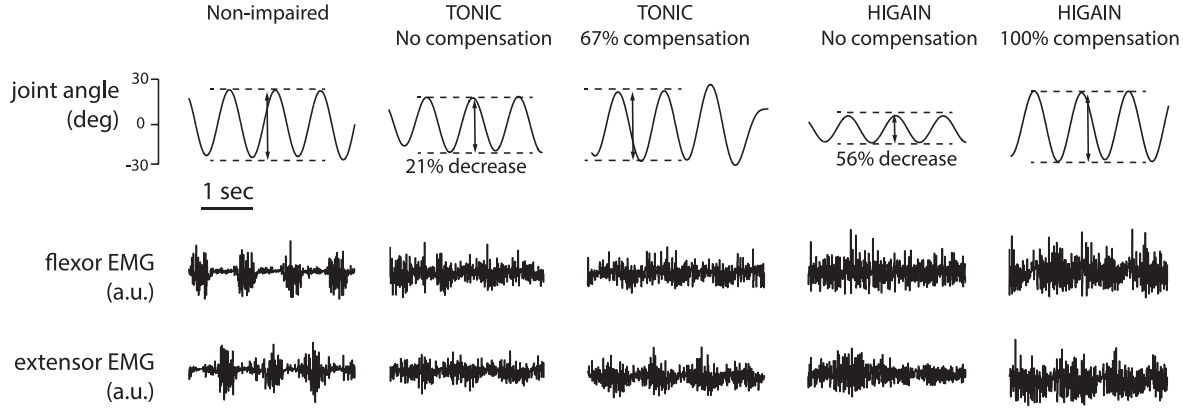

Figure 9. Dystonia models predict that the range of motion in voluntary arm-swing movement should be reduced in dystonia; with certain level of compensation by increasing the voluntary command, the range of movement can be recovered. In the non-impaired condition, the joint was voluntarily swinging at 1 Hz with approximately 50° range of movement; the muscles are activated using alternating descending commands at 1 Hz as depicted in figure 1 and thus generate alternating EMG bursts. In the TONIC model, we maintained the level and frequency of the 1 Hz voluntary command, but added a tonic input with 80% of the peak-to-peak magnitude of the voluntary command. This reduces the movement range by 21%, which can be recovered by compensating the voluntary command by 67% of its original magnitude. In the HI-GAIN model, a 4.7 times increase in the synaptic gain of cortical neuron pool decreased the movement range by 56%, which can be recovered by compensating the voluntary command by 100%.

result from elevated LLSR involving primarily position-dependent (slowly adapting) afferents.

4.2. Rationale of model validation

When validating our models against human data, we focused on whether varying a single parameter in the model could produce a wide range of outcome measures compatible with the human data. We did not, however, focus on the exact matching between emulated time series and human data. This is because dystonia has been known as a disease with high inter-patient variability, and data from humans are limited. As a result, we argue it is not that useful if the model aims at matching exactly to the physiological signals of human patients. Take experiment 1 as an example, the power of the HI-GAIN model comes from its ability to explain the phase angle of any of the six patients using the same disease structure. Given more data from patients with secondary dystonia, the range of outcome measures also provides an experimentally testable criterion to distinguish different models.

4.3. Thoughts on the two mechanisms of elevated LLSR

Either abnormality modeled by the two models can lead to elevated LLSR. This is important because intuitively it might appear that only the HI-GAIN model would increase the gain of the LLSR. Our results suggest that changes in threshold due to tonic drive can also achieve similar effects. It is possible that there is more than one mechanism of dystonia, and this points out that there may be multiple causes of similar phenomenology. For example, disorders of intrinsic excitability of motor areas (genetic or chemical) can produce dystonia, but so could disorders of other areas that project to

primary motor areas. Therefore dystonia could result either from disorders of primary motor areas or from disorders of upstream areas, yet the manifestations will be difficult to distinguish on clinical grounds (although there are some differences).

Another utility of the modeling TONIC and HI-GAIN models is that they potentially represent different etiologies. In particular, a multiplicative increase in the loop gain (HI-GAIN model) cannot be implemented by an additive component added to the system, such as a leak in the transmembrane current. In consequence, if the experimental data favors one model over the other, it suggests that the clinical diagnosis of dystonia should reflect the characteristics of the favored model, e.g. progressively increased phase angles or delayed relaxation.

4.4. Factors that may affect the phase angle in experiment 1

Since phase angle is determined by the nonlinearity of a system and also its intrinsic delay, several factors in our neuromorphic emulation could directly affect the phase angle, including (1) the relative contribution between the primary (group Ia, both velocity- and position-dependent) and secondary (group II, mainly position-dependent) afferents of spindle, (2) the relative contribution between short- and long-latency pathway, and (3) the overall loop delay. Within the range from 180° to 0°, higher activity in the primary spindle fiber makes the system more velocity-dependent, resulting in lower phase angles; while higher activity in the secondary spindle fiber increases the phase angle. When scanning the intensity of dystonia we keep the activity similar between primary and secondary spindle afferents. When constructing the boundary condition of emulation, the secondary spindle fibers are removed such that the system is the least position-dependent, which theoretically provides the smallest phase angle, and vise versa for the largest phase angle. The effect of loop delay on the phase angle is much weaker compared to fiber type, therefore loop delay is not considered when building the boundary conditions.

4.5. EMG response during muscle shortening

Two patients (subject 4 and 5, van Doornik *et al* 2009) are excluded from the model since their positive phase angles suggest their muscles were activated by muscle shortening. This 'shortening reaction' is mostly seen in Parkinsonism, but it is uncommon in normal afferented muscles since most of the proprioceptive spinal pathways are excitatory. Inhibitory pathways (e.g. Renshaw cells or reciprocal inhibition connections) are capable of reducing the EMG but usually not producing shortening reactions. One possible explanation for these two subjects is that there exists an overflow from the opposing muscle. Our models do not include inhibitory pathways or motor overflow. More experimental and modeling work is required to explain the positive joint angles attested in these two patients.

4.6. Advantage and limitation of neuromorphic hardware emulation

The use of hardware emulation provides a powerful tool for understanding the minimal model complexity for producing normal and pathological behaviors. It is clear that the hardware emulation could not accommodate all the physiological details involved in real behavior. For example, we emulated the closed-loop reflex of a joint with spinal pathways and simplified transcortical pathways. The cortical neuron pool only includes a single layer of 128 neurons that are far from the realistic anatomy in the primary sensory and motor cortices. Nevertheless, this simplified reconstruction of the cortex allows us to adjust only the long-latency component of the proprioceptive feedback independent from the functioning short-latency loop. Compared to studying the real biological system, hardware emulation is advantageous since it allows a precise and physiologically tenable intervention on the non-impaired system.

It is also an important issue whether our simplification of the sensorimotor system would lead to a locally correct conclusion that, however, cannot be generalized. It has been found that reflex of shoulder joint is concurrently modulated by the elbow joint (Pruszynski *et al* 2011). This suggests that a standalone reflex loop of a single joint, as modeled in this study, may overlook the contribution from adjacent loops that would increase the LLSR and eventually worsen dystonia. On the contrary, our model did not include inhibitory pathways such as reciprocal inhibition, Renshaw cells, etc, which suggests that a more complex model may decrease LLSR and thus alleviate dystonia. In short, the model is *sufficient* to create some features of dystonia, but there could certainly be other contributors. It is unlikely that the inclusion of more joints would prevent the occurrence of dystonia, but it is likely to change its nature. It would be important to model dystonia in a multi-joint scenario.

5. Conclusion

In summary, we have shown through neuromorphic emulation that there are at least two possible mechanisms of cortical abnormality that could cause increased LLSR and result in the clinical phenomenon of dystonia. While an emulation of this type does not prove that this is the mechanism of dystonia, it does provide evidence that a mechanism of this type is sufficient to cause the clinical features of dystonia, and is therefore worthy of further study. We hope that these results provide both insight and guidance for future clinical studies to test whether reducing the LLSR may alleviate symptoms of dystonia.

Acknowledgments

The authors are grateful for support from the James S McDonnell Foundation. Research reported in this publication was also supported in part by the National Institute of

Neurologic Disorders and Stroke (R01-NS069214), and the National Institute of Arthritis and Musculoskeletal and Skin Diseases (R01-AR052345) of the National Institutes of Health. The content is solely the responsibility of the authors and does not necessarily represent the official views of the National Institutes of Health.

References

Air E L, Ostrem J L, Sanger T D and Starr P A 2011 Deep brain stimulation in children: experience and technical pearls *J. Neurosurgery: Pediatrics* **8** 566–74

Breakefield X O, Blood A J, Li Y, Hallett M, Hanson P I and Standaert D G 2008 The pathophysiological basis of dystonias *Nat. Rev. Neurosci.* **9** 222–34

Capaday C, Forget R, Fraser R and Lamarre Y 1991 Evidence for a contribution of the motor cortex to the long-latency stretch reflex of the human thumb *J. Physiol.* **440** 243–55

Carpaneto J, Micera S, Galardi G, Micheli A, Carboncini M C, Rossi B and Dario P 2004 A protocol for the assessment of 3D movements of the head in persons with cervical dystonia *Clin. Biomech.* **19** 659–63

Ceballos-Baumann A O 1994 Overactivity of primary and associated motor areas in secondary hemi-dystonia (SHD) due to thalamic or basal ganglia lesions: a PET study *Mov. Disorders: Official J. Mov. Disorder Soc.* **9** 238

Colton C A, Brown C M, Czapiga M and Vitek M P 2002 Apolipoprotein-E allele-specific regulation of nitric oxide production *Ann. New York Acad. Sci.* **962** 212–25

DeLong M R and Wichmann T 2007 Circuits and circuit disorders of the basal ganglia *Arch. Neurology* **64** 20–4

Edwards M J, Huang Y Z, Mir P, Rothwell J C and Bhatia K P 2006 Abnormalities in motor cortical plasticity differentiate manifesting and nonmanifesting DYT1 carriers *Mov. Disorders: Official J. Mov. Disorder Soc.* **21** 2181–6

Edwards M J, Huang Y Z, Wood N W, Rothwell J C and Bhatia K P 2003 Different patterns of electrophysiological deficits in manifesting and non-manifesting carriers of the DYT1 gene mutation *Brain: J. Neurology* **126** 2074–80

Emonet-Denand F, Laporte Y, Matthews P B and Petit J 1977 On the subdivision of static and dynamic fusimotor actions on the primary ending of the cat muscle spindle *J. Physiol.* **268** 827–61

Evarts E V and Tanji J 1976 Reflex and intended responses in motor cortex pyramidal tract neurons of monkey *J. Neurophysiol.* **39** 1069–80

Fuglevand A J, Winter D A and Patla A E 1993 Models of recruitment and rate coding organization in motor-unit pools *J. Neurophysiol.* **70** 2470–88

Ghez C, Gordon J and Hening W 1988 Trajectory control in dystonia *Adv. Neurology* **50** 141–55

Hallett M 2011 Neurophysiology of dystonia: The role of inhibition *Neurobiology Disease* **42** 177–84

Hashimoto T, Naito K, Kitazawa K, Imai S and Goto T 2010 Pallidotomy for severe tardive jaw-opening dystonia *Stereotactic Funct. Neurosurgery* **88** 105–8

Henneman E, Somjen G and Carpenter D O 1965 Functional significance of cell size in spinal motoneurons *J. Neurophysiol.* **28** 560–80

Hill A V 1938 The heat of shortening and dynamics constants of muscles *Proc. R. Soc.* B **126** 136–95

Imer M, Ozeren B, Karadereler S, Yapici Z, Omay B, Hanagasi H and Eraksoy M 2005 Destructive stereotactic surgery for treatment of dystonia *Surgical Neurology* **64** S89–94

Izhikevich E M 2003 Simple model of spiking neurons *IEEE Trans. Neural Netw. Publication of the IEEE Neural Netw. Counc.* **14** 1569–72

Kojovic M, Parees I, Kassavetis P, Palomar F J, Mir P, Teo J T, Cordivari C, Rothwell J C, Bhatia K P and Edwards M J 2013 Secondary and primary dystonia: pathophysiological differences *Brain: J. Neurology* **136** 2038–49

Krauss J K 2010 Surgical treatment of dystonia *Eur. J. Neurology: Official J. Eur. Fed. Neurological Soc.* **17** 97–101

Krutki P, Ciechanowicz I, Celichowski J and Cywinska-Wasilewska G 2008 Comparative analysis of motor unit action potentials of the medial gastrocnemius muscle in cats and rats *J. Electromyogr. Kinesiology: Official J. Int. Soc. Electrophysiol. Kinesiology* **18** 732–40

Kukke S N and Sanger T D 2011 Contributors to excess antagonist activity during movement in children with secondary dystonia due to cerebral palsy *J. Neurophysiol.* **105** 2100–7

Lebiedowska M K, Gaebler-Spira D, Burns R S and Fisk J R 2004 Biomechanic characteristics of patients with spastic and dystonic hypertonia in cerebral palsy *Arch. Phys. Med. Rehabil.* **85** 875–80

Lee R G, Murphy J T and Tatton W G 1983 Long-latency myotatic reflexes in man: mechanisms, functional significance, and changes in patients with Parkinson's disease or hemiplegia *Adv. Neurology* **39** 489–508

Matthews P B 1991 The human stretch reflex and the motor cortex *Trends Neurosci.* **14** 87–91

McIntyre C C, Savasta M, Kerkerian-Le G L and Vitek J L 2004 Uncovering the mechanism(s) of action of deep brain stimulation: activation, inhibition, or both *Clin. Neurophysiol.: Official J. Int. Fed. Clin. Neurophysiol.* **115** 1239–48

Mileusnic M P, Brown I E, Lan N and Loeb G E 2006 Mathematical models of proprioceptors: I. Control and transduction in the muscle spindle *J. Neurophysiol.* **96** 1772–88

Morimoto C, Distaso J A, Cheney J J, Reinherz E L and Schlossman S F 1984 Cellular interaction between subsets of T8 population for maximal suppression of antigen-specific antibody response *Cell. Immunology* **88** 75–84

Murray W M, Delp S L and Buchanan T S 1995 Variation of muscle moment arms with elbow and forearm position *J. Biomech.* **28** 513–25

Niu C M, Nandyala S K and Sanger T D 2014 Emulated muscle spindle and spiking afferents validates VLSI neuromorphic hardware as a testbed for sensorimotor function and disease *Frontiers Comput. Neurosci.* **8** 141

Palmer E and Ashby P 1992 Evidence that a long latency stretch reflex in humans is transcortical *J. Physiol.* **449** 429–40

Prescott I A, Dostrovsky J O, Moro E, Hodaie M, Lozano A M and Hutchison W D 2013 Reduced paired pulse depression in the basal ganglia of dystonia patients *Neurobiology Disease* **51** 214–21

Pruszynski J A, Kurtzer I, Nashed J Y, Omrani M, Brouwer B and Scott S H 2011 Primary motor cortex underlies multi-joint integration for fast feedback control *Nature* **478** 387–90

Quartarone A, Bagnato S, Rizzo V, Siebner H R, Dattola V, Scalfari A, Morgante F, Battaglia F, Romano M and Girlanda P 2003 Abnormal associative plasticity of the human motor cortex in writer's cramp *Brain: J. Neurology* **126** 2586–96

Ridding M C, Sheean G, Rothwell J C, Inzelberg R and Kujirai T 1995 Changes in the balance between motor cortical excitation and inhibition in focal, task specific dystonia *J. Neurology Neurosurgery Psychiatry* **59** 493–8

Rodriguez I, Gila L, Malanda A, Gurtubay I G, Mallor F, Gomez S, Navallas J and Rodriguez J 2007 Motor unit action potential duration: I. Variability of manual and automatic measurements *J. Clinical Neurophysiol.: Official Publication of the Am. Electroencephalographic Soc.* **24** 52–8

Sanger T D 2011 Distributed control of uncertain systems using superpositions of linear operators *Neural Comput.* **23** 1911–34

Sanger T D, Delgado M R, Gaebler-Spira D, Hallett M, Mink J W, Task Force on ChildhoodMotor D 2003 Classification and definition of disorders causing hypertonia in childhood *Pediatrics* **111** e89–97

Scheidt R A and Ghez C 2007 Separate adaptive mechanisms for controlling trajectory and final position in reaching *J. Neurophysiol.* **98** 3600–13

Trompetto C, Avanzino L, Marinelli L, Mori L, Pelosin E, Roccatagliata L and Abbruzzese G 2012 Corticospinal excitability in patients with secondary dystonia due to focal lesions of the basal ganglia and thalamus *Clin. Neurophysiol.: Official J. Int. Fed. Clin. Neurophysiol.* **123** 808–14

van Doornik J, Kukke S and Sanger T D 2009 Hypertonia in childhood secondary dystonia due to cerebral palsy is associated with reflex muscle activation *Mov. Disorders: Official J. Mov. Disorder Soc.* **24** 965–71

Vidailhet M *et al* 2005 Bilateral deep-brain stimulation of the globus pallidus in primary generalized dystonia *New England J. Medicine* **352** 459–67

Weise D, Schramm A, Stefan K, Wolters A, Reiners K, Naumann M and Classen J 2006 The two sides of associative plasticity in writer's cramp *Brain: J. Neurology* **129** 2709–21